Instruments and Experimental Techniques, Vol. 43, No. 3, 2000, pp. 305–318. Translated from Pribory i Tekhnika Eksperimenta, No. 3, 2000, pp. 5–18.
Original Russian Text Copyright © 2000 by Khabibullin, Grigor'ev, Ivashkin, Kudenko, Mineev, Khotyuzhev.

NUCLEAR EXPERIMENTAL TECHNIQUES

CsI(Tl)-Calorimeter Calibration with Positive-Kaon Decay Products

M. M. Khabibullin, M. P. Grigor'ev, A. P. Ivashkin, Yu. G. Kudenko, G. Y. Mineev, and A. N. Khotyuzhev

Institute for Nuclear Research, Russian Academy of Sciences, pr. Shestidesyatiletiya Oktyabrya 7a, Moscow, 117312 Russia

Received March 22, 2000

Abstract—The CsI(Tl) calorimeter was calibrated in the KEK-E246 experiment with $K_{\mu 3}$- and K_{e3}-positive-kaon decays. The following calorimeter parameters were obtained: an energy resolution (σ) of 4.1% for E = 242.5 MeV, a π^0 invariant-mass resolution (σ) of 5.6%, and an angular resolution (σ) of 3.1°.

1. INTRODUCTION

The electromagnetic calorimeter on the basis of CsI(Tl) crystals is used to detect photons in the E246 experiment which is conducted with the proton synchrotron (Japan) and aimed at measuring the T-violating transverse muon polarization (P_T) in a decay $K^+ \longrightarrow \pi^0\mu^+\nu(K_{\mu 3})$. The first experimental results are presented in [1]. A layout of the experiment is shown in Fig. 1.

Positive kaons with a 660-MeV/c momentum, identified with the Cherenkov detector *3* [2], traverse the degrader *4* and are stopped in the active target *5*. The target (Fig. 2) is composed of 256 scintillating fibers *1* with a cross section of 5 × 5 mm^2, surrounded by 12 fiducial counters *2* and the scintillation ring hodoscope *3*. Muons from a $K_{\mu 3}$ decay of the stopped kaon are detected with the active target, the ring hodoscope, and a system of proportional chambers. The μ^+ momentum is determined in the course passage through a sector of the 12-sector superconducting toroidal magnet *9* (B = 0.9 T) and the system of three multiwire proportional chambers C_1–C_3 in each sector (side view is Fig. 1). The muon, which came to a stop in the polarimeter, decays through the mode $\mu^+ \longrightarrow e^+\nu\bar{\nu}$. The thus produced positrons are detected by the scintillation counters located symmetrically about the median plane of each magnet sector. The readings of these positron counters N_L and N_R (the numbers of hits, respectively, of the counters located on the left and on the right of the median plane) are used to evaluate the T-odd polarization that is extracted from the asymmetry $A_T = (N_L - N_R)/(N_L + N_R)$, summed over all 12 sectors. Neutral pions are detected by the CsI(Tl) calorimeter situated at the center of the toroidal magnet.

The complete reconstruction of the $K_{\mu 3}$-decay kinematics is an important feature of the experiment (1). This feature helps optimize the sensitivity to P_T and efficiently suppress the systematic errors, owing to the azimuthal detector symmetry and the use of the double ratio, i.e., the comparison of the asymmetry for two types of events with π^0 moving back and forth relative to the initial kaon beam.

2. CsI(Tl) CALORIMETER

The *detector* for neutral π^0-mesons (Fig. 3) is symmetric to the azimuthal and polar directions. It consists of two parts (those in front of and behind the kaon beam), each containing ten types of CsI(Tl) crystals (produced by the Single Crystals Factory, Kharkov, Ukraine) [3–5]. The total number of crystals is 768. Each crystal (Fig. 4) is shaped as a truncated pyramid with an apex angle of 3.5° (the length is 25 cm, and the average cross sections are 3 × 3 and 6 × 6 cm^2), is wrapped with a diffusion reflector *1* (120-μm-thick Millipore OSWP00010) and encased in a thin aluminum container *2* with 100-μm-thick walls. Since the calorimeter is placed in a strong magnetic field, semiconductor photodiodes (S-3204-03 and S-3584-05 by Hamamatsu, Japan) are used as photodetectors.

The signal from the photodiode *3* goes to the charge-sensitive preamplifier *4* located near the photodiode, and, then, to the main amplifier. The analog signal from the spectrometric output of this amplifier is digitized with the analog-to-digital converter made to the TKO standard [6]. The time signal arrives at the time-to-digital converter of the same standard. The detector's electronics is described in detail in [7].

The CsI(Tl) modules form a barrel structure with 12 holes for muons to pass into the magnet sectors. The modules embrace about 75% of a full space angle of 4π (Figs. 2, 5).

3. CALORIMETER CALIBRATION

The main K^+ decay modes are presented in the table. The feasibility of recording two-particle $K_{\mu 2}$- and K_{e3}

0020-4412/00/4303-0305$25.00 © 2000 MAIK "Nauka/Interperiodica"

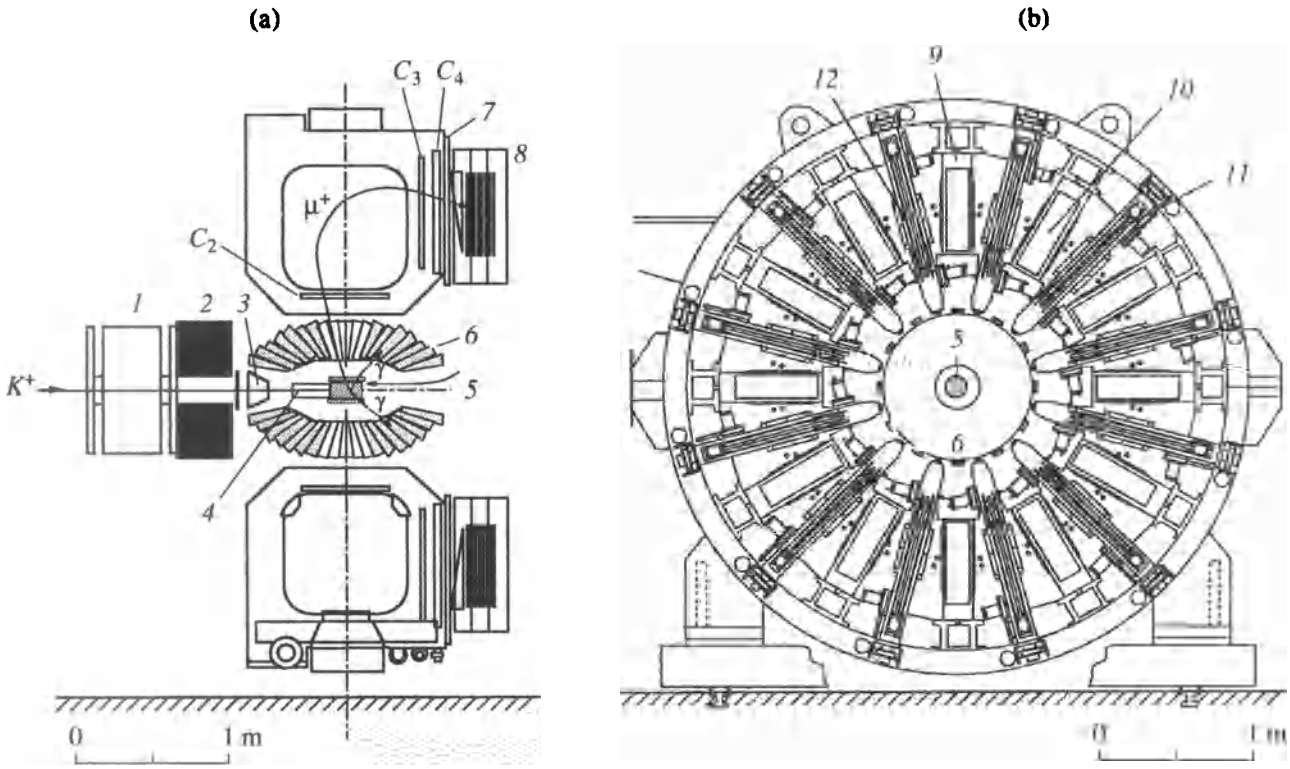

Fig. 1. Schematic diagram of the E246 experimental setup: (a) side view and (b) front view. (*1*) Focusing magnet; (*2*) collimator; (*3*) Cerenkov counter; (*4*) kaon degrader; (*5*) active target; (*6*) CsI(Tl) calorimeter; (*7*) time-of-flight counter; (*8*) polarimeter; (*9*) sector of the toroidal magnetic spectrometer; (*10*) muon moderator; (*11*) positron counter; (*12*) magnet winding; and (C_2–C_4) multiwire proportional chambers.

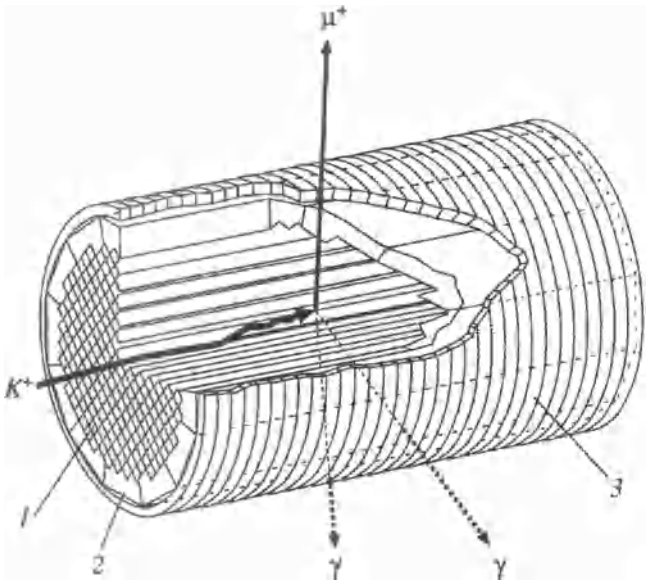

Fig. 2. Schematic diagram of the active target: (*1*) scintillating fiber with rectangular cross section (5×5 mm^2); (*2*) fiducial counters; and (*3*) ring hodoscope. A $K_{\mu 3}$ decay is presented.

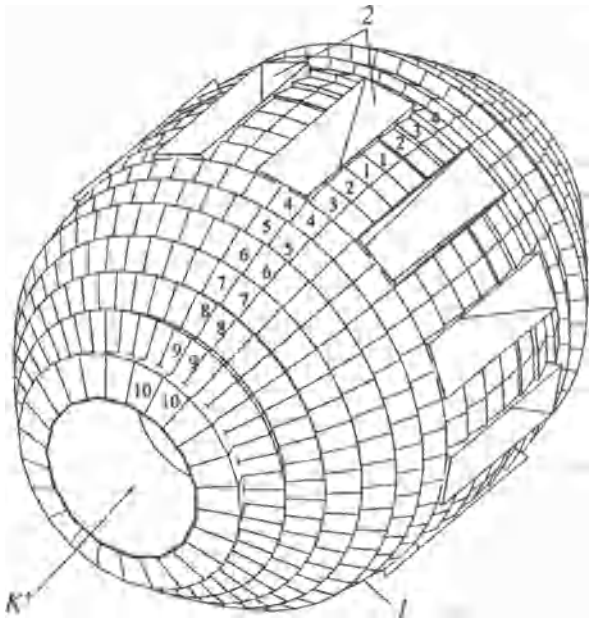

Fig. 3. Diagram of the neutral-pion detector: (*1*) CsI(Tl) modules forming a barrel structure; and (2) holes for muon escape (there are 12 holes in all, according to the number of toroidal-magnet sectors). The numbers 1–10 correspond to the crystal type.

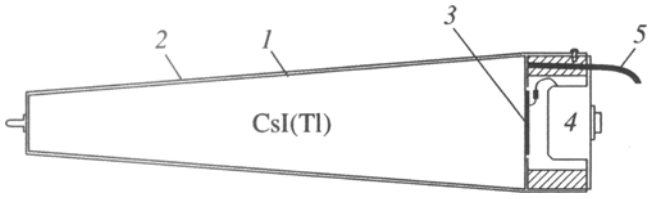

Fig. 4. View of the CsI(Tl) module: (1) radiator; (2) aluminum container; (3) photodiode; (4) preamplifier; and (5) fiber.

decays with a CsI(Tl) detector without resort to the toroidal magnet has made it possible to use these decay muons for CsI(Tl)-module calibration.

3.1. Calibration with Muons from a $K_{\mu 2}$ Decay

A muon with a kinetic energy T_μ = 152 MeV, produced in the active target as a result of $K_{\mu 2}$ decay of the kaon at rest, traverses the scintillating fibers and the fiducial counters and reaches a CsI(Tl) module. The module length (25 cm) is sufficient for muon to deposit its entire energy and come to a rest inside this crystal. Then, with the knowledge of the energy lost by the muon in the target (fibers + fiducial counters + passive material), it is possible to calculate the muon energy deposited in the given crystal:

$$dE_{csi} = T_\mu - dE_{aux}, \qquad (1)$$

where T_μ is the initial kinetic energy of the muon, and dE_{aux} is the muon energy deposited in the target, which is a sum of the losses in the fibers (dE_{fib}) and fiducial counters (dE_{fc}). The calibration factor for this CsI(Tl) module is found from Eq. (1):

$$C_i = dE_{csi}/(A - P)_i, \qquad (2)$$

where i = 1, ..., 768 is the module number, A and P are the amplitude and pedestal of the appropriate ADC.

For the values of dE_{csi} to be correct, it is necessary to discard the events in which even one of the following conditions is satisfied: (i) the muon traverses an adjacent crystal ("skewed" trajectories), which results in additional energy loss outside the module; (ii) the muon comes to a rest in this crystal and then decays (τ_μ = 2.2 μs), and the positron produced inevitably releases its electromagnetic shower in this module, thus increasing the energy deposition.

Each case leads to over- and underestimation, respectively, of the calibration factor for this module, thus resulting in incorrect calculation of the photon energy and the π^0 invariant mass.

3.2. Event Selection for Calibration

The electronic calibration trigger includes the kaon identification with the Cerenkov detector, kaon stop in the target, and the presence of a signal in the CsI(Tl). Detecting events from an in-flight K^+ decay is avoided by introducing a ~15-ns time delay.

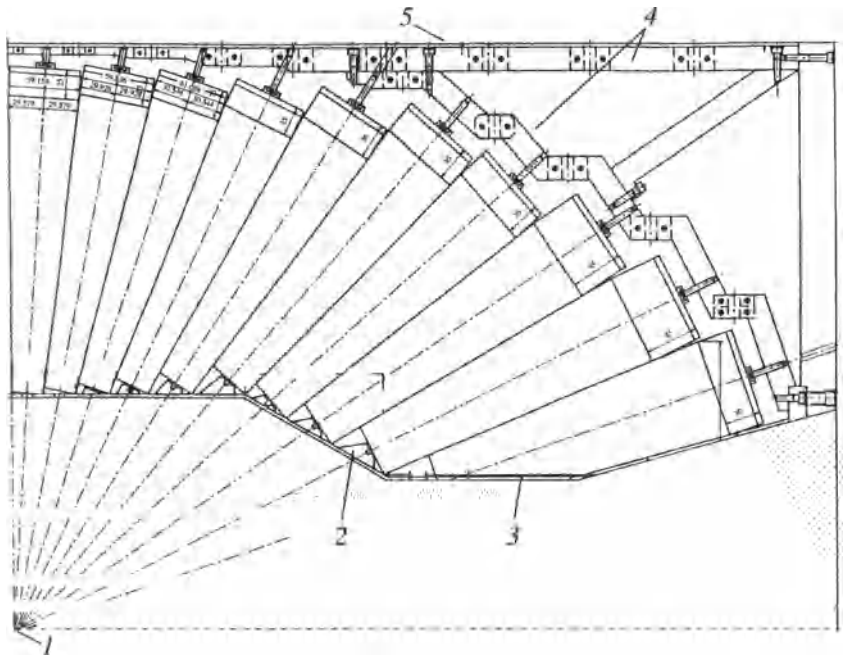

Fig. 5. Cross-sectional view of the lateral-plane detector (only the downstream sector of the detector is shown): (1) plane-layer corner of the detector; (2) detector support frame; (3) barrier shell; (4) longitudinal stiffening ribs; and (5) conductor shell.

The K^+-decay modes (June 1998)

Decay	Relative probability of decay, %	Energy of decay products, MeV
$K^+ \longrightarrow \mu^+ \nu_\mu (K_{\mu 2})$	63.51	$T_\mu = 152.4$
$K^+ \longrightarrow \pi^+ \pi^0 (K_{\pi 2})$	21.16	$T_{\pi^+} = 110.6$
		$T_{\pi^0} = 108.5$
$K^+ \longrightarrow \pi^0 \mu^+ \nu_\mu (K_{\mu 3})$	3.18	$T_\mu^{max} = 118.9$

Only the events meeting the following criteria are selected for subsequent analysis: (1) The energy deposited in a fiber (the stop point of the kaon) is high (>5 MeV). (2) Only one track originating at the stop point of the kaon (the trace of a muon from the kaon decay) is found in the plane of the target cross section (*XY* plane). (3) Only one CsI(Tl) module was fired in the calorimeter within the signal-integration time (~2 μs). (4) The fired CsI(Tl) module is an extension of the muon track in the target (in the *XY* plane).

To suppress the events (I, II) described in Section 3.1, the following two conditions are added: (5) The energy deposited in the modules surrounding the fired crystal is negligibly small:

$$(A - P)_i \leq 10, \quad (i = 1, \ldots, 8), \qquad (3)$$

where the ADC channels correspond to about 0.6 MeV in each of the eight modules surrounding the central one. (6) The energy is released in the given CsI(Tl) module within a short time interval ($\Delta t = 28$ ns).

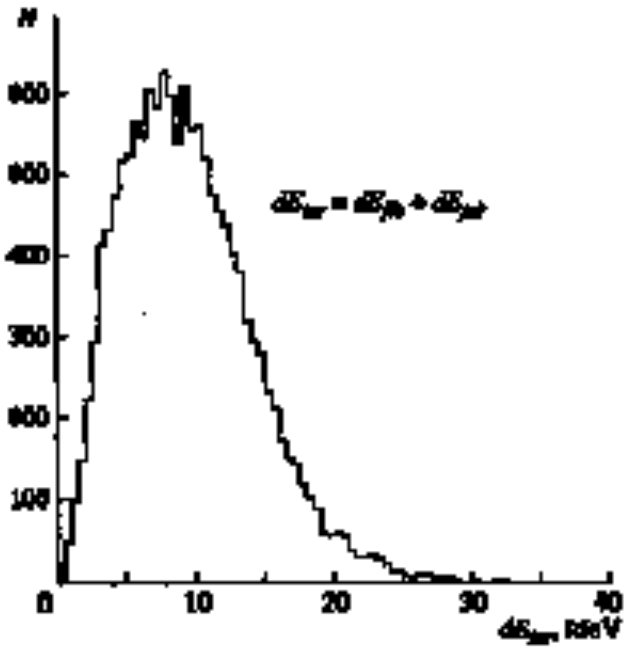

Fig. 6. The energy deposited in a charged particle in the target dE_{dep}, which is a sum of the losses in the fibers dE_p and fibrid counters $dE_{\mu p}$.

3.3. Energy Deposited in the Target

For each of the 256 fibers and 12 fibrid counters, the energy scale is calibrated against the losses of minimum-ionizing particles. Then the losses in each of the calibrated counters are added in order to obtain the total energy deposited in the target by a muon from a $K_{\mu 2}$ decay. An energy spectrum dE_{dep} is shown in Fig. 6. The peak position of about 7 MeV corresponds to the energy loss of the particle emitted from the central fiber of the target, and the high-energy spectral region is associated with the particles crossing the target at small angles with the beam direction. The charged-particle trajectory is determined from the fired fibers in the plane of the target cross section; this helps determine the direction where the operative CsI(Tl) module should be sought.

Note that the use of this method for determining the muon energy deposited in the target gives rise to an additional error of ~1 MeV, it is caused by the fact that the fibers where the kaon is stopped are discarded, since it is only from within portions of energy are deposited in these counters by the muon and the kaon itself.

3.4. Calibration Spectra

Using formula (2) and taking into account the requirements in Section 3.2, a histogram of coefficients is produced for each CsI(Tl) module in the course of data analysis. Each histogram is then approximated by a Gaussian function with a mean which is the best estimate for the calibration factor of the relevant CsI(Tl) module. Through the detector's configuration, the histograms for inner- and tenth-type modules have the smallest statistic; therefore, these histograms are smoothed before the approximation. The basic phase of the detector calibration ends in determination of 768 calibration factors.

The calibration result is shown in Fig. 7. The factors obtained are used to estimate the energy release in a given CsI(Tl) module for the calorimeter middle part (the fifth to eighth types of crystals) in view of the loss in the target and the requirements in Section 3.2. The most probable value of 152 MeV is not considered, because exactly this value is used in Eq. (2), it is important that the decay-positron spectrum in the 152–200-MeV range (the total muon and positron energy deposited in the module) is greatly suppressed, which confirms the validity of the event-selection criteria in use. A small peak near 113 MeV is due to positive pions from the $K_{\pi 2}$ decay. The effective suppression of these events is associated with the severe criteria for their selection (see Section 3.2), which require operation of only one CsI(Tl) module in the calorimeter. For the $K_{\pi 2}$ decay, this requirement means simultaneous escape of both

photons from the π^0 decay into the muon or beam holes in the calorimeter.

4. VERIFICATION OF THE CALIBRATION WITH EVENTS OF $K_{\pi 2}$ DECAY

A $K_{\pi 2}$ decay is a unique process for electromagnetic-calorimeter calibration, because its products are a neutral pion with a total energy $E_{\pi^0} = 245.6$ MeV and a positive pion with a kinetic energy $T_{\pi^+} = 108.5$ MeV. The positive pion then decays into a muon with a kinetic energy $T_{\mu^+} = 4.2$ MeV and a neutrino.

The neutral pion decays into two photons with a known total energy. This fact can also be used for calorimeter calibration with the so-called matrix method, determining the calibration factors for individual modules by solving a system of linear equations. However, this approach has produced far worse results than the $K_{\pi 2}$ method, because of the "leakage" of the electromagnetic shower through the muon and beam holes.

Nevertheless, $K_{\pi 2}$ decay is used to verify the coefficients that have already been obtained, since both π^0 and π^+ can be detected with the calorimeter. For these events to be extracted, it is necessary that there be three different clusters of activated CsI(Tl) modules in the calorimeter; in addition, the direction towards one of the three clusters should be an extension of the track in the target (a cluster of crystals that have detected a charged particle).

4.1. Detection of a π^0 from a $K_{\pi 2}$ Decay

After extracting the cluster that has detected a charged particle, the particle energy is estimated using the individual calibration factors obtained for each cluster module; then, the energy deposited by a charged particle in the target is added. The total energy spectrum for the calorimeter middle part is presented in Fig. 5. A narrow peak near 112 MeV corresponds to a π^+ that has stopped in the calorimeter and decayed, producing a positive muon which has added its kinetic energy to the muon cluster. Positrons from the decays of muons that have come to a stop in the crystals also contribute to the spectrum.

The spectral peak position (112.0 MeV) is displaced from the kinematically evaluated value (112.7 MeV) by 0.7 MeV, which has within the accuracy in determining the energy loss in the target (see Section 3.3). It is important that the energy of a charged particle from the other decay (π^+ from the $K_{\pi 2}$ decay), estimated using the calibration factors obtained with the $K_{\pi 2}$ decay, happened to be correct. This proper calibration and the calorimeter linearity are thereby confirmed, at least, for charged particles with up to 160-MeV energy.

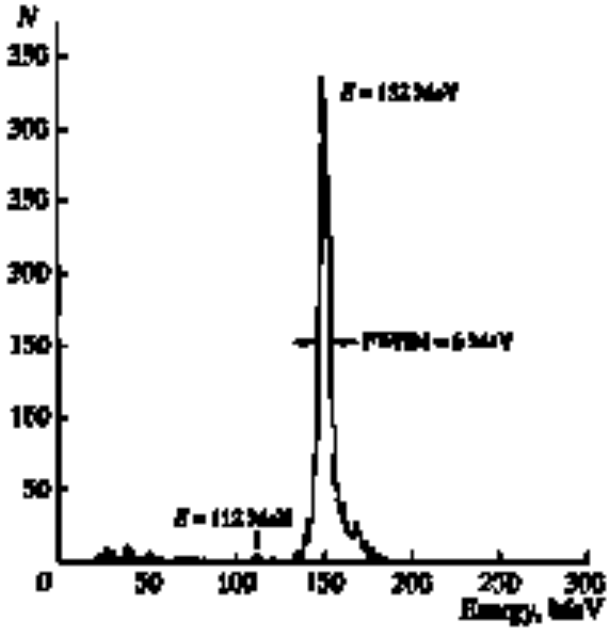

Fig. 5. The energy spectrum measured with the CsI(Tl) crystal located at the calorimeter middle part (M) in eight types of modules in view of the energy release in the target. The peak position at about 112 MeV corresponds to the kinetic energy of muons from $K_{\pi 2}$ decays. The high-energy spectral region (up to 300 MeV) corresponds to the initial gamma spectrum resulting from muon decays in the crystal. At low energies, the spectrum corresponds mainly to electrons (MIPs). A small peak near 112 MeV is due to positive pions from $K_{\pi 2}$ decay.

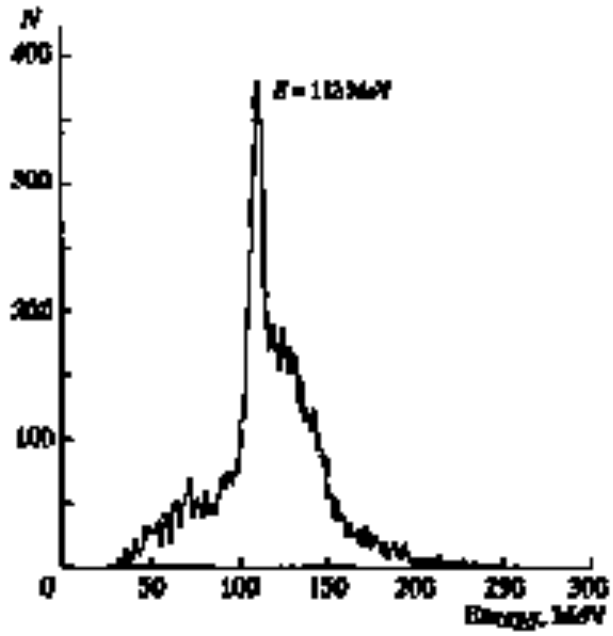

Fig. 6. The energy spectrum, measured with the cluster of crystals that have detected a charged particle, in view of the energy deposited in the target. The energy values near the peak (112 MeV) corresponds to the sum of the kinetic energies of π^+ from $K_{\pi 2}$ decay (108.5 MeV) and μ^+ from π^+ decay (4.2 MeV), stopped in the muon cluster.

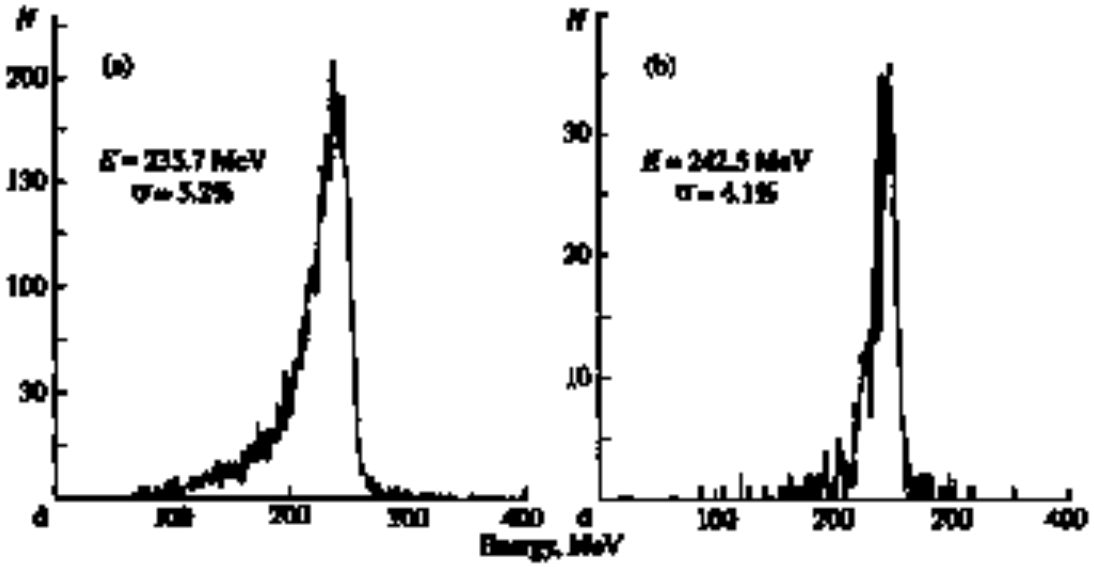

Fig. 8. The sum of the energy of two photons from $K_{\pi 2}$ decay, detected by two clusters of 25 CsI(Tl) modules: (a) all events in the π^0 detector and (b) only those events when the photons have been detected outside the beam holes.

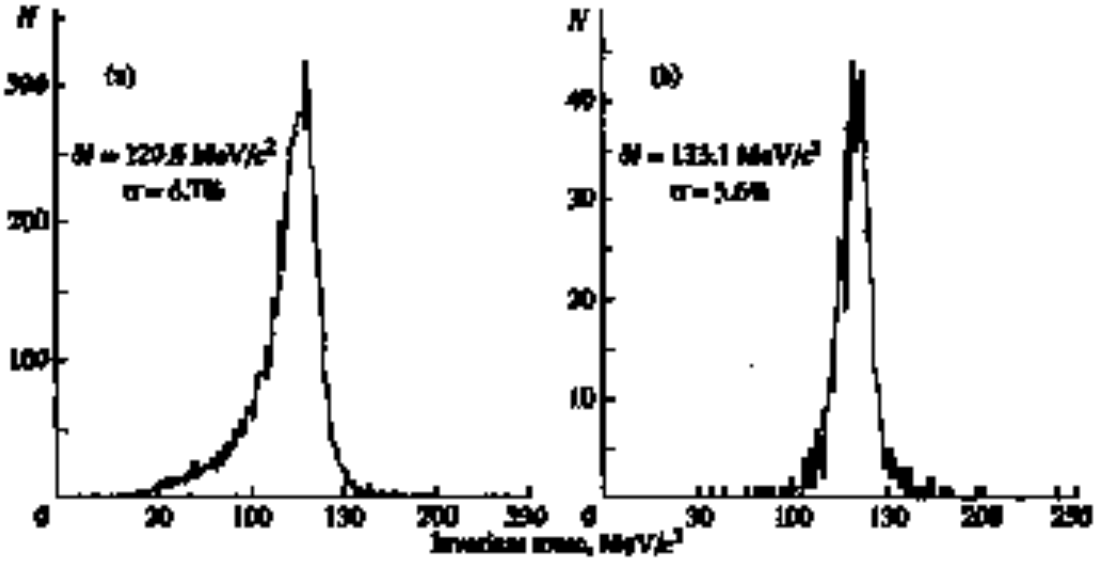

Fig. 10. The π^0 invariant-mass spectrum, $M_{\gamma\gamma}$, of $K_{\pi 2}$-decay events for two clusters of 25 CsI(Tl) modules: (a) all events in the π^0 detector and (b) only those events when the photons have been detected outside the beam holes.

We note the difference between the spectra for $K_{\pi 2}$ (Fig. 7) and $K_{\mu 2}$ decays (Fig. 8). In the second case, there is a continuous spectrum from the right of the sharp peak (112 MeV). It looks like a "hillock" up to about 160 MeV and corresponds to the positron spectrum from muon decays with a standard value of the Michel parameter. This spectrum is not observed in the first case when stringent requirements have been specified for both the response time and cluster size. The background of random coincidences is also present in Fig. 8, which is due to relatively soft criteria for event selection.

4.2. *Detection of a π^0 from a $K_{\pi 2}$ Decay*

Figure 9 shows the total-energy spectra for two photons from a π^0 decay, detected by the CsI(Tl) calorimeter. Each photon is detected by a cluster of 25 crystals (5 × 5), using the entire calorimeter (Fig. 9a) and neglecting the events when the center of the electromagnetic shower falls at the crystals bordering on the detector holes (Fig. 9b). Comparison of these spectra demonstrates the effect of electromagnetic-shower "leakage" through the holes in the calorimeter. The spectrum in Fig. 9a is asymmetric, with a low-energy

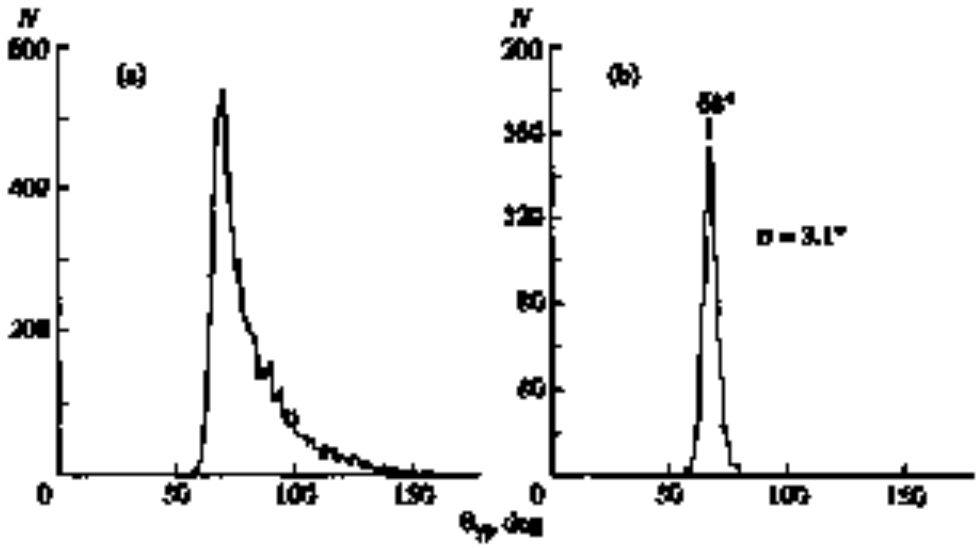

Fig. 11. The distribution of the angle between two emitted photons from the π^0 decay for the K_{e3} mode: (a) all K_{e3} events are presented; (b) only those events with symmetric π^0 decay are shown when $(E_{\gamma 1} - E_{\gamma 2})/(E_{\gamma 1} + E_{\gamma 2}) \leq 0.1$.

tail, until the peak position (235.7 MeV) is shifted by about 7 MeV from the peak in Fig. 9b. The most probable value of 242.5 MeV (Fig. 9b) corresponds to a fraction of 96.7% of the initial energy of neutral pion from K_{e3} decay, which is explained by the electromagnetic-shower "leakage," primarily, through the rear surfaces of the crystals. Therefore, according to Fig. 9b, the energy resolution σ of the calorimeter for the two-photon energy $E = 242.5$ MeV is 4.1%.

The important calorimeter parameter used to identify a photon pair from the neutral-pion decay is the invariant-mass resolution $M_{\gamma\gamma} = \sqrt{2E_{\gamma 1}E_{\gamma 2}(1 - \cos\theta_{\gamma\gamma})}$, where $E_{\gamma 1}$ and $E_{\gamma 2}$ are the photon energies and $\theta_{\gamma\gamma}$ is the angle between them.

If a photon detector is ideal, $M_{\gamma\gamma}$ must be equal to the neutral-pion mass ($m_{\pi^0} = 135$ MeV/c^2). However, by virtue of the finite calorimeter resolution and the presence of a background instead of a single line, we obtain a spectrum of $M_{\gamma\gamma}$ values. Two spectra of this kind are shown in Fig. 10 for two 25-crystal clusters (5 × 5), when all clusters (Fig. 10a) and only the calorimeter part outside the holes (Fig. 10b) are considered.

Like the total energy, the comparison of both invariant-mass spectra graphically demonstrates the effect of electromagnetic-shower "leakage" through the calorimeter holes. The peak position of the spectrum in Fig. 10b lies near 129.6 MeV/c^2, and the spectrum is highly asymmetric and sloping towards smaller masses. The peak position in Fig. 10b is displaced towards a value of 133.1 MeV/c^2, and the spectrum becomes more symmetric. Thus, the calorimeter has an invariant-mass resolution (σ) of 5.6%.

The angular resolution is determined as follows. According to the kinematic equations, the angle between two emitted photons $\theta_{\gamma\gamma}$ is the smallest (=67°) when $E_{\gamma 1} = E_{\gamma 2}$. Figure 11 shows two distributions in the angle $\theta_{\gamma\gamma}$: for all K_{e3}-decay events (Fig. 11a) and for the case when the photon energies, measured with the calorimeter, are very close: $(E_{\gamma 1} - E_{\gamma 2})/(E_{\gamma 1} + E_{\gamma 2}) \leq 0.1$ (Fig. 11b). The last one helps estimate the angular characteristics of the calorimeter: the spectrum peak corresponds to 68°, which is in agreement with the kinematically expected value, and the angular resolution (σ) is 3.1°.

Thus, verification with the events of K_{e3} decay confirms the correctness of the calibration factors obtained with muons from $K_{\mu 2}$ decay.

5. CONCLUSION

We have described the procedure for calibrating the CsI(Tl) calorimeter in the KEK-E246 experiment, using particles from positive-kaon $K_{\mu 2}$ and K_{e3} decays. The following calorimeter parameters were obtained from the calibration: an energy resolution (σ) of 4.1% for a 242.5-MeV energy of two photons, a π^0-invariant-mass resolution (σ) of 5.6%, and an angular resolution (σ) of 3.1°.

ACKNOWLEDGMENTS

We thank all participants in the E246 experiment for help in conducting the sessions.

This work was supported by the Russian Foundation for Basic Research, project no. 99-02-17814.

REFERENCES

1. Abe, M., Aoki, M., Arai, I., *et al.*, *Phys. Rev. Lett.*, 1999, vol. 83, p. 4253.
2. Grigor'ev, M.P., Dement'ev, D.V., Ivashkin, A.P., *et al.*, *Prib. Tekh. Eksp.*, 1998, no. 6, p. 65.
3. Kudenko, Yu.G. and Imazato, J., *KEK Report*, 1992, no. 92-15.
4. Grigor'ev, M.P., Dement'ev, D.V., Ivashkin, A.P., *et al.*, *Prib. Tekh. Eksp.*, 1996, no. 2, p. 18.
5. Dementyev, D.V., Grigoriev, M.P., Ivashkin, A.P., *et al.*, *Nucl. Instrum. Methods Phys. Res., Sect. A*, 2000, vol. 440, p. 151.
6. Ohska, T.K., TKO Specification, *Preprint KEK*, 1985, no. 85-10.
7. Kudenko, Yu.G., Mineev, O.V., and Imazato, J., *Nucl. Instrum. Methods Phys. Res., Sect. A*, 1998, vol. 411, p. 437.